MODEL REDUCTION TECHNIQUES FOR THE SIMULATION OF PARTICLE POPULATIONS IN FLUID FLOW

M. Krasnyk[1], M. Mangold[2]
[1] Otto-von-Guericke-Universität Magdeburg, Germany, [2] Max-Planck-Institut für Dynamik komplexer technischer Systeme, Magdeburg, Germany

Corresponding author: M. Krasnyk, Otto-von-Guericke-Universität Magdeburg, Lehrstuhl für Automatisierungstechnik und Modellbildung, Universitätsplatz 2, D-39106 Magdeburg, Germany, Tel.: +49 391 6110-377, mailto: miha@mpi-magdeburg.mpg.de

Abstract. Crystallization processes are characterized by a close interaction between particle formation and fluid flow. A detailed physical description of these processes leads to complicated high order models whose numerical solution is challenging and expensive. For advanced process control and other model based online applications, reduced order models are required. In this work, a reduced model for a urea crystallizer is developed, using the method of moments for the internal coordinate and proper orthogonal decomposition for the external coordinate. Simulations are carried out to compare the reduced model with the detailed reference model.

1 Introduction

Crystallization denotes the formation of solid particles from a solute dissolved in a liquid solvent. Crystallization is one of the most important processes in chemical and pharmaceutical industry. The majority of chemical products and even more than 90% of pharmaceutical agents are produced in crystalline form. Furthermore, crystallization is an intermediate step used for purification in many chemical production processes.

Usually crystal properties like characteristic size or shape determine the quality of crystalline products. Therefore the main task of design and control of crystallization processes is to generate particle populations with desired property distributions. Property distributions change due to various physical phenomena like nucleation, *i.e.* formation of new crystals, crystal growth, breakage or agglomeration. All these effects depend strongly on the interaction between fluid flow and particle phase. A realistic mathematical model of a crystallization process must account for transport processes in the liquid phase and in the solid phase as well as for the coupling between both phases. The model has to describe fluid dynamic effects in up to three space coordinates or external coordinates and in addition the development of particle populations along one or several internal coordinates like *e.g.* the characteristic particle size. The resulting high-dimensional models are very complex. Their numerical solution is challenging and a subject of current research [1]. For many applications in the field of model based process control such detailed models are hardly suitable. Instead, there is a need for low order models capable of predicting the key features of a crystallization process in the relevant operation window with reasonable accuracy. This work aims at developing such models.

The model reduction process consists of lumping in the external coordinates as well as in the internal coordinates. For both sets of coordinates reduction techniques are available in literature. For the internal coordinates, the method of moments and its extensions have been widely used [2]. For the external coordinates, reduced-basis approximation or Proper Orthogonal Decomposition (POD)[3] has been applied successfully, starting from the pioneering work by Sirovich [4]. It proved to be useful for solving inverse problems or for optimal control with applications in a wide range of different fields, like nondestructive evaluation of delamination, modelling of dispersion of pollutants, assessment of welding quality [5], simulation of heat transfer problems [6], or control of nonlinear flow problems [7] or fuel cells [8]. Different methods for improvements of the POD model reduction have been proposed recently, e.g. via variational multiscale stabilization [9] or adaptive proper orthogonal decomposition for the solution of reaction-diffusion problems [10].

This contribution discusses model reduction for the example of a spatially two-dimensional model of a urea crystallizer. The reference model contains incompressible Navier-Stokes equations for the liquid phase. A population balance equation (PBE) describes the particle phase. Details on the reference model are given in the next section. The model reduction strategy is presented in Section 3. Section 4 compares simulation results of the reduced model and the reference model.

2 Reference model

2.1 Model equations

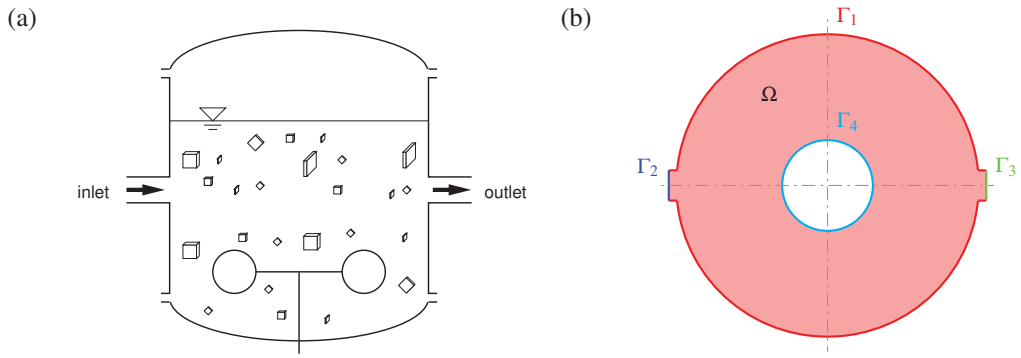

Figure 1: (a) Scheme of a continuous crystallizer; (b) simplified 2D geometry of the crystallizer seen from top.

Figure 1 (a) gives a schematic view of a continuous industrial crystallizer. Fresh liquid feed with seeding urea crystals enters the stirred tank reactor from the left. The seeding crystals grow inside the reactor. At the product outlet on the right-hand side of the reactor, a mixture of liquid and crystals is continuously removed. To model the process a simplified two-dimensional geometry is used that is shown in Figure 1 (b). The simplified geometry neglects spatial gradients in vertical direction, and the stirrer is modeled as a rotating cylinder in the center of the system. To derive model equations for this process, further simplifying assumptions are made:

- The crystallizer is operated under isothermal conditions.
- The crystals are needles with a time-independent cross-sectional area $\bar{A}$ [11].
- A simple kinetic expression for the size-independent growth rate of the crystals is taken from [12]
- Particle nucleation, breakage, attrition and agglomeration are not taken into account.

The crystallizer's fluid phase is described by the incompressible Navier-Stokes equations. The continuity equation and the momentum balance that are expressed by the following system of partial differential equations:

$$\begin{aligned} \nabla \cdot u &= 0 && \text{in } (0,T]\times\Omega, \\ \rho \dot{u} + \rho(u\cdot\nabla)u &= -\nabla p + \mu\Delta u && \text{in } (0,T]\times\Omega, \end{aligned} \tag{1}$$

where $u := (u\ v)^T$ is the vector of flow velocities in $x-$ and in $y-$ direction, p is the pressure, μ and ρ are the fluid viscosity and the fluid density, respectively. The concentration c of the solute is described by a scalar convection-diffusion equation that results from a component mass balance:

$$\dot{c} + u\cdot\nabla c = D_c\Delta c - r_g(c,f) \quad \text{in } (0,T]\times\Omega \tag{2}$$

D_c is the diffusion coefficient. The term r_g stands for the mass transfer between fluid phase and particle phase due to crystal growth. It can be written as

$$r_g(c,f) = \frac{\rho_U \bar{A}}{M_A} G \int_0^\infty f dl \tag{3}$$

where ρ_U is the density of the crystals, M_A is their molar mass, and f is the number density function of the crystal population.

The particle phase is modeled by a population balance for the particle size distribution that accounts for crystal growth and convective transport of crystals in space:

$$\frac{\partial f}{\partial t} + u\cdot\nabla f = -G\frac{\partial f}{\partial L} \quad \text{in } (0,T]\times\Omega\times[0,\infty) \tag{4}$$

The population balance depends on time and space and in addition on the particle size coordinate L.

The growth rate [12] is a power function

$$G = \begin{cases} 6.04\times10^3 \left(\frac{c-c_{eq}}{c_{eq}}\right)^{1.65} \mu\text{m/s}, & c > c_{eq}, \\ 0, & c \leqslant c_{eq}, \end{cases} \tag{5}$$

where c_{eq} is the saturation concentration.

Boundary conditions in space subject to the geometry in Figure 1 (b) are as follows. The boundary Γ_1 has a no slip flow field with an isolation of c and f. The internal boundary Γ_2 is a uniformly rotating wall with a velocity ω that represents a simplified impeller. This imposes the following condition on the velocity field : $u = (-\omega_y, \omega_x)^T$. Γ_2 is an isolation for c and f. The inlet Γ_3 has a parabolic velocity profile $u = \left(4u^{in}s(1-s), 0\right)^T$. The inlet liquid concentration of the solute at Γ_3 is given by $c = c^{in}$. Further, the feed contains particle seeds with length zero. This leads to the boundary condition $f|_{L=0} = f_0^{in}$. The outlet Γ_4 presents convective outflow of the fluid. The initial conditions are zero velocity field $u(x,0) = 0$ and zero concentration and particle size distribution.

A simplified description of the particle phase follows if the size distribution function is replaced by its moments μ_k defined as

$$\mu_k = \int_0^\infty L^k f dL \quad \text{for } k = 0, 1, \ldots \tag{6}$$

Inserting the definition (6) into the population balance (4) results in the following closed equation system for the first two moments:

$$\begin{array}{rcl} \dot{\mu}_0 + u \cdot \nabla \mu_0 & = & 0 \\ \dot{\mu}_1 + u \cdot \nabla \mu_1 & = & G\mu_0 \end{array} \tag{7}$$

An obvious physical interpretation can be given for the moments μ_0 and μ_1: μ_0 denotes the total number of crystals at one point in space, the ratio μ_1/μ_0 is a measure for the average crystal size.

The use of moments reduces the rate of mass consumption due to crystal growth r_g to

$$r_g = \frac{\rho_U \bar{A} G}{M_A} \mu_0. \tag{8}$$

More complicated population balances including additional phenomena, like, particle breakage or agglomeration will give a non-closed set of the moments and will require additional treatment like e.g. the application of the quadrature method of moments, where moments are approximated by the Gaussian quadrature [2, 13].

2.2 Simulation results

Comsol Multiphysics [14] is used to simulate the described crystallizer model and to obtain reference solutions for the reduced model that will be derived in the following. Parameters used in the numerical simulation are presented in Table 1.

Table 1: Numerical simulation parameters

Parameter	Value	Units
μ	10^{-3}	kg/m/s
ρ	10^3	kg/m^3
D_c	0.75×10^{-9}	m^2/s
ρ_U	1335	kg/m^3
M_A	60.07	g/mol
$\bar{A}$	4×10^{-13}	m^2
c_{eq}	10.47	mol/l
c^{in}	11	mol/l
f_0^{in}	10^{10}	1/m^3
ω	$2\pi \cdot 10^{-4}$	1/s
u^{in}	10^{-4}	m/s
R_1	10	cm
R_2	3	cm
D^A_{c,μ_0}	10^{-5}	m^2/s
$D^A_{\mu_1}$	10^{-7}	m^2/s

The numerical simulation shows that the fluid flow achieves a steady state in 1 second of the simulation time, the concentration c and the zeros moment μ_0 become perfectly mixed in 20 seconds of the simulation time, and the first moment μ_1 attains the steady state in 40 seconds. Figure 2 illustrates the development of μ_1 in time by some

snapshots. One can see that initially crystals with nonzero length exist only close to the inlet on the left-hand side. The seeding crystals fed to the system move with the fluid flow in a counter-clockwise direction and gradually gain size. After about 8 s a steady state profile has been achieved. The biggest crystals occur slightly above the feed point because the crystals in this area have the biggest residence time in the reactor.

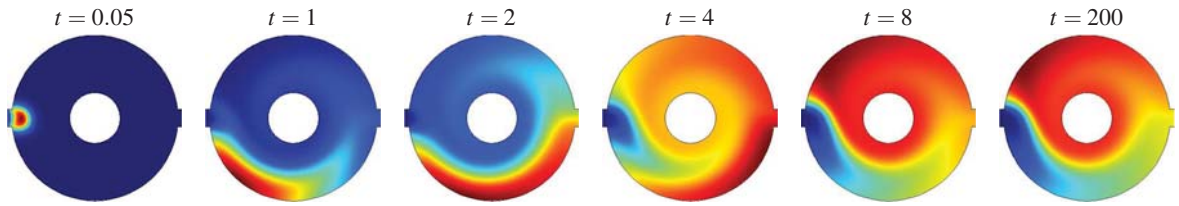

Figure 2: Development in time of the first moment μ_1 with $u^{in} = 10^{-4}$ m/s

3 Model reduction in space by Proper Orthogonal Decomposition

In this work, Proper Orthogonal Decomposition (POD) has been used to achieve a model reduction in spatial coordinates. POD has its roots in statistical analysis and is a technique used to reduce multidimensional data sets to lower dimensions for analysis, it is also named principal component analysis or Karhunen-Loève transform [15].

The velocity field u, the concentration c, and the moments μ_0 and μ_1 are approximated with a finite Galerkin projection

$$\begin{gathered} u = \begin{pmatrix} u \\ v \end{pmatrix} = \bar{u} + u', \quad \bar{u} = \langle u \rangle, \quad u' = \sum_{i=1}^{M_{uv}} a_i^{uv} \begin{pmatrix} \sigma_i^u \\ \sigma_i^v \end{pmatrix}, \quad u'|_{\partial\Omega} = 0, \\ c = \langle c \rangle + \sum_{i=1}^{M_c} a_i^c \sigma_i^c, \quad \mu_k = \langle \mu_k \rangle + \sum_{i=1}^{M_{\mu_k}} a_i^{\mu_k} \sigma_i^{\mu_k}, \quad \text{and } \langle f \rangle = \lim_{T\to\infty} \frac{1}{T} \int_0^T f \, \mathrm{d}t \end{gathered} \tag{9}$$

with time dependent coefficients a_i^j and space dependent modes σ_i^j that represent orthonormal bases for suitable solution spaces.

The spatial basis functions are obtained from the proper orthogonal decomposition of a reference simulation of the detailed model that has been described in the previous section. In POD the basis functions $\sigma^j(x)$ are chosen to maximize the following expression

$$\frac{\langle (\sigma^j(x), u(x,t))^2 \rangle}{(\sigma^j(x), \sigma^j(x))} \stackrel{!}{=} \max \tag{10}$$

with the inner product $(f,g) = \int_\Omega fg \, \mathrm{d}\Omega$. The maximization problem corresponds to a constrained optimization problem for

$$J[\sigma] = \langle (\sigma, u)^2 \rangle - \lambda((\sigma,\sigma) - 1) \stackrel{!}{=} \max \tag{11}$$

where λ is a Lagrange multiplier. An extremum σ must satisfy

$$\frac{\mathrm{d}}{\mathrm{d}\delta} J[\sigma + \delta\psi]|_{\delta=0} = 2[\langle (u,\psi)(\sigma,u) \rangle - \lambda(\sigma,\psi)] \stackrel{!}{=} 0 \tag{12}$$

This is equivalent to solving the integral equation

$$\int_\Omega \langle u(x,t)^T u(\xi,t) \rangle \sigma(\xi) \, \mathrm{d}\xi = \lambda \sigma(x). \tag{13}$$

So in terms of the POD the optimal basis is composed of eigenfunctions $\{\sigma^j\}_{j=1}^\infty$ of the integral equation (13), whose kernel is the averaged autocorrelation function

$$R(x,\xi) := \langle u(x,t)^T u(\xi,t) \rangle. \tag{14}$$

The main advantage of the POD is that it produces the best linear representation for an ensemble of functions or flowfields (snapshots).

In [4] a procedure called the method of snapshots was developed that reduces the cost of the solution to that of an eigenvalue problem of size equal to the number of modes we intend to use. The method of snapshots uses the fact that the autocorrelation function can be expressed as

$$R(x,\xi) = \lim_{M\to\infty} \frac{1}{M} \sum_{i=1}^{M} u_i^T(x) \cdot u_i(\xi) \tag{15}$$

where $u_i(x) = u(x, i\tau)$ is referred to as a snapshot and τ is the sampling time which should be greater than the correlation time. For the finite number of snapshots M the kernel $R(x,\xi)$ will be degenerated and eigenfunctions will correspond to a linear combination of the snapshots

$$\sigma^i(x) = \sum_{k=1}^{M} \alpha_k^i u_k(x). \tag{16}$$

With this assumption, the integral eigenvalue problem (13) in finite-dimensional space is transformed into an eigenvalue problem

$$\mathscr{R}_{ij}\alpha^i = \lambda_i \alpha^i \tag{17}$$

for the symmetric $M \times M$-matrix

$$\mathscr{R}_{ij} = \frac{1}{M}(u_i(x), u_j(x)) \tag{18}$$

and the basis functions are

$$\sigma^i(x) = \sum_{k=1}^{M} \alpha_k^i u_k(x). \tag{19}$$

The described model reduction process has been implemented in Matlab [16]. It comprises the following steps:

1. Snapshots are generated by solving the reference model in Comsol and exporting the results to Matlab.
2. Mean values $\bar{w} = \langle w \rangle$ and normalized snapshots $w' = w - \bar{w}$ are computed, where $w = \{u, c, \mu_0, \mu_1\}$.
3. Computation of matrices for $1 \leqslant i, j \leqslant n_{snap}^w$

$$R_{ij}^w = \frac{1}{n_{snap}^w}(w_i', w_j') \quad \text{with } (\varphi, \psi) = \int_\Omega \varphi^T \psi \, \mathrm{d}x \tag{20}$$

4. Computation of the basis functions $\sigma^w = w' V^w$, where V^w are the first n_{eef}^w eigenvectors of R^w
5. Normalization of σ^w
6. Computation of coefficient matrices for the reduced model, *e.g.*, for u

$$\begin{aligned} A_{kij}^u &= (\sigma_k^u, \sigma_i^u \cdot \nabla \sigma_j^u) \\ B_{ki}^{u,1} &= (\sigma_k^u, \bar{u} \cdot \nabla \sigma_i^u) \qquad B_{ki}^{u,2} = (\sigma_k^u, \sigma_i^u \cdot \nabla \bar{u}) \qquad B_{ki}^{u,3} = (\sigma_k^u, \Delta \sigma_i^u) \\ C_k^{u,1} &= (\sigma_k^u, \bar{u} \cdot \nabla \bar{u}) \qquad C_k^{u,2} = (\sigma_k^u, \Delta \bar{u}) \end{aligned} \tag{21}$$

7. Computation of the initial values via projection of $w'(0)$ to the reduced solution spaces

$$a_k^w(0) = (\sigma^w, w'(0)), \qquad 1 \leqslant k \leqslant n_{eef}^w \tag{22}$$

As a result of the reduction process, one obtains the following low-order ODE model:

$$\begin{aligned} \rho \dot{a}_k^u &= -\rho \left[A_{kij}^u a_i^u a_j^u + (B_{ki}^{u,1} + B_{ki}^{u,2}) a_i^u + C_k^{u,1} \right] + \mu \left[B_{ki}^{u,3} a_i^u + C_k^{u,2} \right] \\ \dot{a}_k^c &= -\left[A_{kij}^c a_i^u a_j^c + B_{ki}^c a_i^c + C_{ki}^c a_i^u + E_k^c \right] + (D_c + D_c^A)(F_k^c + H_{ki}^c a_i^c) - (\sigma_k^c, r_g(c, \mu_0)) \\ \dot{a}_k^{\mu_0} &= -\left[A_{kij}^{\mu_0} a_i^u a_j^{\mu_0} + B_{ki}^{\mu_0} a_i^{\mu_0} + C_{ki}^{\mu_0} a_i^u + E_k^{\mu_0} \right] + D_{\mu_0}^A (F_k^{\mu_0} + H_{ki}^{\mu_0} a_i^{\mu_0}) \\ \dot{a}_k^{\mu_1} &= -\left[A_{kij}^{\mu_1} a_i^u a_j^{\mu_1} + B_{ki}^{\mu_1} a_i^{\mu_1} + C_{ki}^{\mu_1} a_i^u + E_k^{\mu_1} \right] + D_{\mu_1}^A (F_k^{\mu_1} + H_{ki}^{\mu_1} a_i^{\mu_1}) + (\sigma_k^{\mu_1}, G(c, \mu_0)) \end{aligned} \tag{23}$$

where the first terms correspond to the correspond to the convective parts of equations, the second parts correspond to diffusive parts, and the last terms present the nonlinear growth parts. In order to increase numerical robustness, additional terms with coefficients D_c^A, $D_{\mu_0}^A$, and $D_{\mu_1}^A$, which infer isotropic artificial diffusion, are included in the reduced model.

4 Simulation results of reduced model

Application of the reduction technique to the reference simulation with $u^{in} = 10^{-4}$m/s delivers a set of mean solutions and normalized basis functions for the model variables u, v, c, μ_0, and μ_1. Figure 3 shows the first basis functions and mean flows for u and v. Mean values for c and μ_0 are constant values c^{in} and f_0^{in}, and for μ_1 the mean value is the steady-state profile at $t = 200$ as shown in Figure 2. Results of the reduced model dynamic

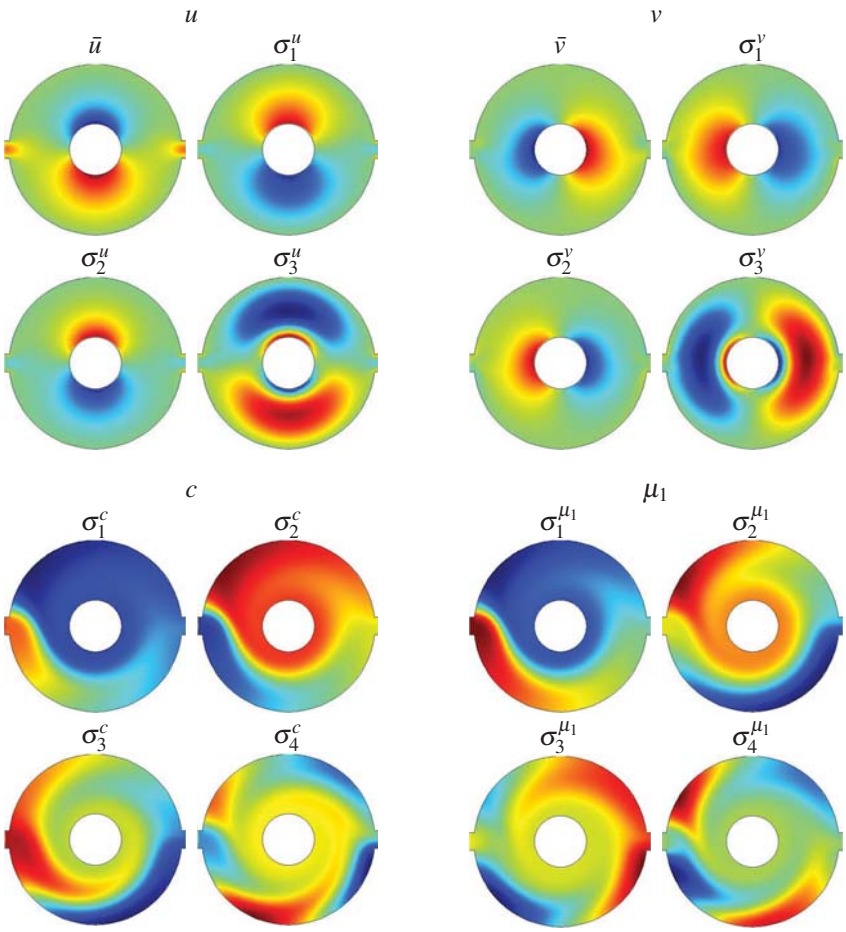

Figure 3: Mean flows for u and v variables, and normalized basis functions σ^u, σ^v, σ^c, and σ^{μ_1}

simulation are shown in Figure 4. One can see that after a transient period all variables of the reduced model go to zero, i.e. the reduced model settles at the correct steady state. The coefficients for the first basis functions can be interpreted as characteristic time constants of the model. For example, the fluid flow reaches the steady state in one second, but c and μ_0 require around 20 seconds and μ_1 needs 40 seconds to attain the steady-state. The relative errors between the reference and the reduced models under transient conditions have been calculated and are shown in Figure 5. For the given set of model parameters the reduction error is bounded in time and less then 1% for all variables. This means that the reduced model is able to reproduce the reference simulation with good accuracy. However, it is more interesting to study the extrapolation qualities of the reduced model, i.e. its ability to predict solutions of the reference model that are not included in the snapshots. In order to apply the reduced model to process control purposes, it is important to have sufficient extrapolation qualities for variations in operation conditions and for variations in physical model parameters that may change under varying operation conditions.

The most important operation parameter of the example system is the inlet flow velocity u^{in}. Therefore, in a first step the quality of the reduced model is tested for varying values of u^{in}. To do this, the reduced model basis functions are obtained from dynamic snapshots of the reference model for a fixed inlet velocity of $u^{in} = 10^{-4}$ m/s. The snapshots are not recomputed, when the inlet velocity changes. However, as the reduced model only computes deviations from a steady state, it is necessary to compute a new steady state reference value from the detailed model, if u^{in} changes. This can be done rather cheaply, as no dynamic simulation is involved. In summary, the

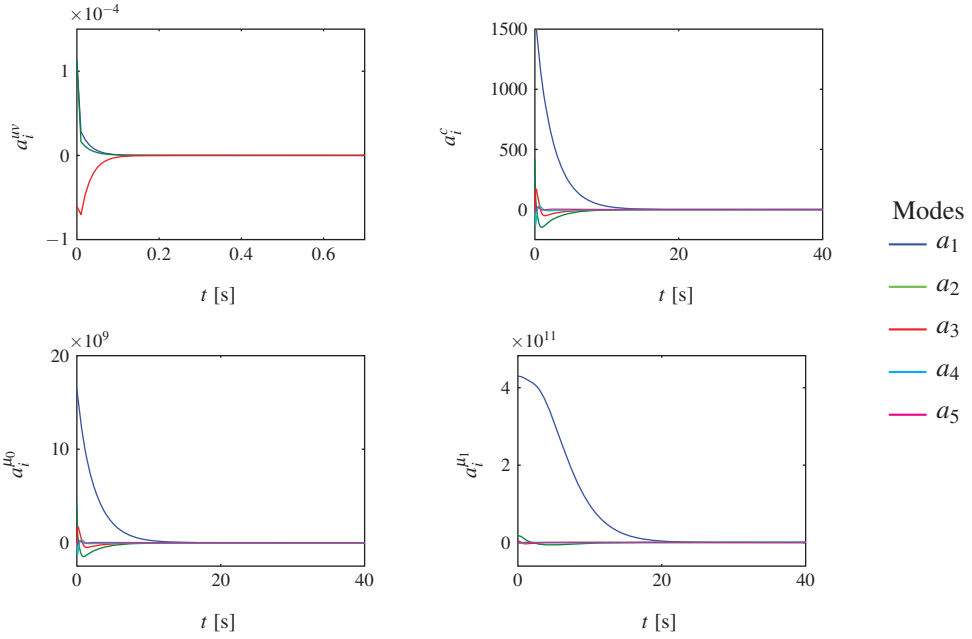

Figure 4: First coefficients a_i of the reduced model dynamic simulation

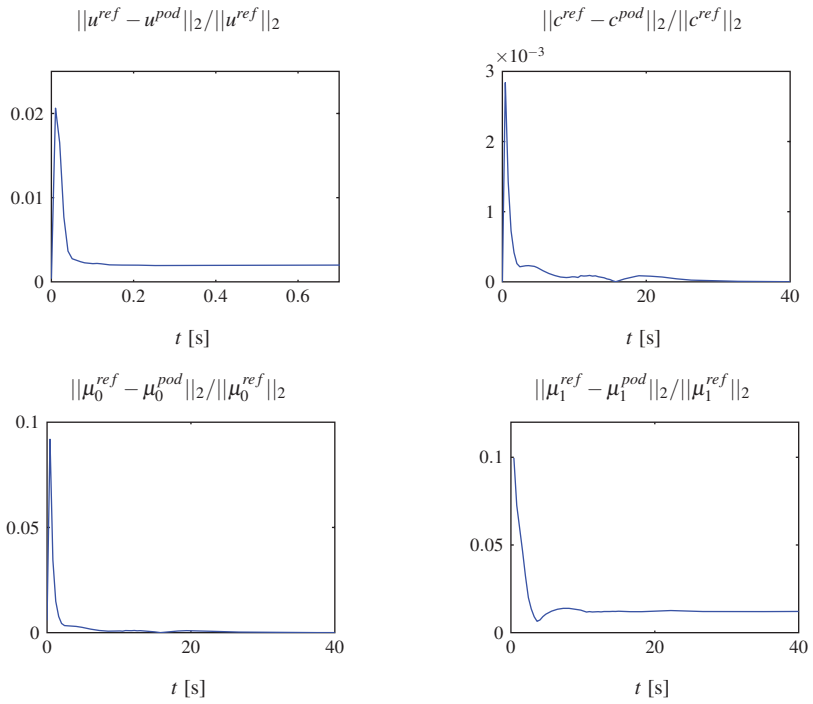

Figure 5: Relative error plots for $u^{in} = 10^{-4}$ m/s

variables of the reduced model can be expressed as

$$w = \bar{w}(u^{in}) + \sum_{i=1}^{M^w} a_i^w \sigma_i^w, \tag{24}$$

with a consequent update of the affected reduced model matrices (21). The reduced model's error dependency on the parameter u^{in} is presented in Figure 6. The plots in Figure 6 show a mean error in the time interval from 0 to 200 seconds. One can see that the reduced model produces very reliable results for u, c, and μ_0, even if the inlet flow velocity is varied over one order of magnitude. However, the sensitivity of the first moment is considerably

bigger. A variation of u_{in} by 10 % produces an error of the reduced model roughly in the same order.

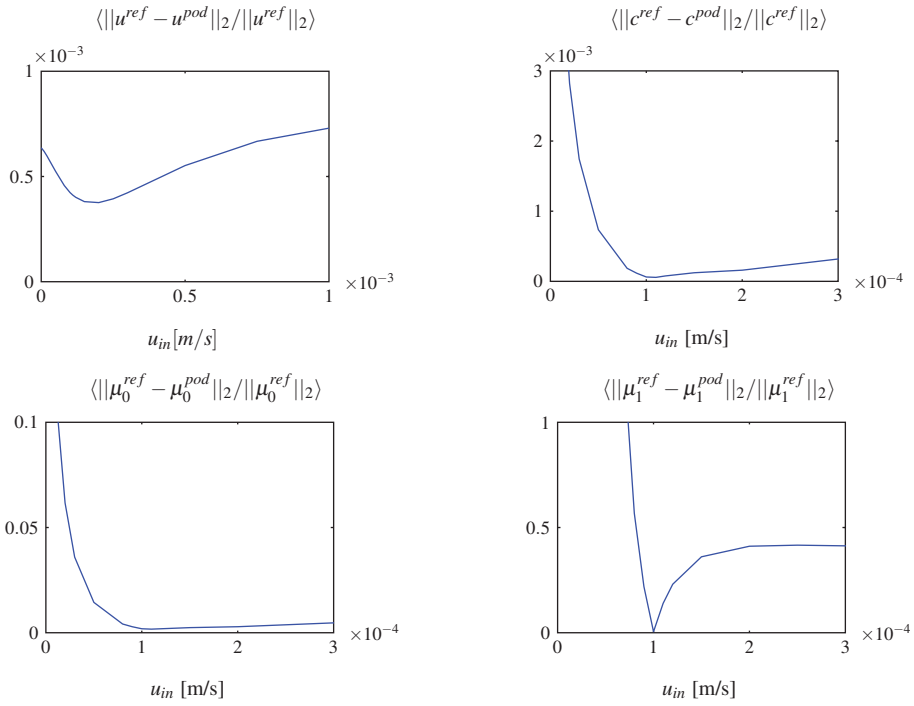

Figure 6: Relative error plots with respect to u^{in}

As an example for a varying physical parameter, the fluid viscosity μ is considered. The fluid viscosity may change, if the particle density increases and the mixture becomes slurry-like. Figure 7 shows that the extrapolation quality of the reduced model is quite good here. The error of all variables increases onlly slightly, when the viscosity is changed. This may be a useful property, when the reduced model is used in a parameter identification environment in order to identify μ.

5 Conclusions

In this contribution a reduced order model for a crystallizer has been developed by using the method of moments and Proper Orthogonal Decomposition. The reduced model shows a good agreement with the reference model. Extrapolation qualities of the reduced model with respect to changes in physical parameters are also quite satisfactory. A reduction in terms of system order by a factor of about 500 is achieved. The reduction of the computation time for simulation is about factor 5, due to the presence of nonlinear terms in the convection-diffusion equations that require numerical quadrature during the simulation of the reduced model. The results indicate that a low number of basis functions can capture the overall system behavior for low Reynolds numbers and sufficiently large diffusion. Smaller diffusion terms will require a larger number of basis functions in order to capture the fine details of spatial features of the convective flow.

As a next step, the model will be extended to include nucleation and breakage as well as a non-constant fluid viscosity that depends on the crystal size. Further, a more efficient treatment of the nonlinear terms is desirable. Possible approaches may be the use of truncated Taylor series for the nonlinear terms, or the application of the empirical interpolation method [17]. The latter method is especially promising for reducing the simulation time because it gives the possibility to calculate all inner products offline.

6 Acknowledgment

This work is supported by a grant from the Federal Ministry of Education and Research (Teilprojekt No. 03KIPAA2)

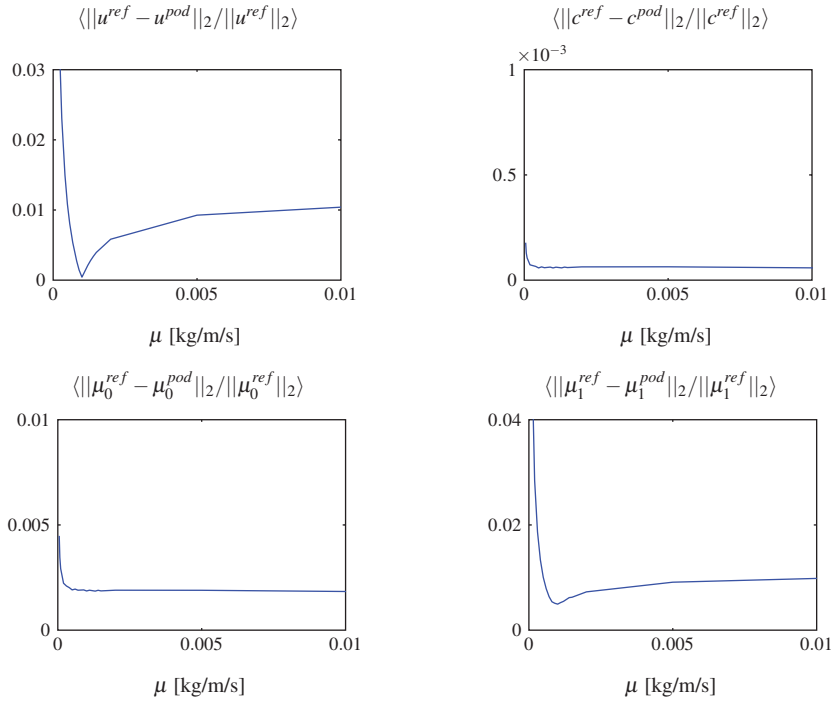

Figure 7: Relative error plots with respect to μ

7 References

[1] Volker John, Teodora Mitkova, Michael Roland, Kai Sundmacher, Lutz Tobiska, and Andreas Voigt. Simulations of population balance systems with one internal coordinate using finite element methods. *Chemical Engineering Science*, In Press, Corrected Proof, 2008.

[2] D. Marchisio, J. Pikturna, Fox R., Virgil R., and Barresi A. Quadratue method of moments for population balance equations. *AIChE Journal*, 49:1266–1276, 2003.

[3] G. Rozza, D. Huynh, and A. Patera. Reduced basis approximation and a posteriori error estimation for affinely parametrized elliptic coercive partial differential equations. *Archives of Computational Methods in Engineering*, 15(3):229–275, 2008.

[4] Lawrence Sirovich. Turbulence and the dynamics of coherent structures. i - coherent structures. II - symmetries and transformations. III - dynamics and scaling. *Quarterly of Applied Mathematics*, 45:561–571, October 1987.

[5] Martin A. Grepl. *Reduced-Basis Approximation and A Posteriori Error Estimation for Parabolic Partial Differential Equations*. PhD thesis, MIT, 2005.

[6] H. M. Park and D. H. Cho. The use of the Karhunen-Loève decomposition for the modeling of distributed parameter systems. *Chemical Engineering Science*, 51(1):81–98, 1996.

[7] Rudibert King, Meline Seibold, Oliver Lehmann, Bernd. Noack, Marek Morzyński, and Gilead Tadmor. Nonlinear flow control based on a low dimensional model of fluid flow. In *Control and Observer Design for Nonlinear Finite and Infinite Dimensional Systems*, pages 369–386. Springer, 2005.

[8] Min Sheng, Michael Mangold, and Achim Kienle. A strategy for the spatial temperature control of a molten carbonate fuel cell system. *Journal of Power Sources*, 162(1):1213–1219, 2006.

[9] M. Bergmann, C.-H. Bruneau, and A. Iollo. Enablers for robust POD models. *Journal of Computational Physics*, In Press, Corrected Proof, 2008.

[10] Michael A. Singer and William H. Green. Using adaptive proper orthogonal decomposition to solve the reaction-diffusion equation. *Applied Numerical Mathematics*, 59(2):272–279, February 2009.

[11] Stefano Piana, Manijeh Reyhani, and Julian D. Gale. Simulating micrometre-scale crystal growth from solution. *Nature*, 438(7064):70–73, November 2005.

[12] R. Davey, W. Fila, and J. Garside. The influence of biuret on the growth kinetics of urea crystals from aqueous solutions. *Journal of Crystal Growth*, 79(1-3, Part 2):607–613, December 1986.

[13] R. Grosch, H. Briesen, W. Marquardt, and M. Wulkow. Generalization and numerical investigation of

QMOM. *AIChE Journal*, 53(1):207–227, 2007.
[14] Comsol multiphysics internet page. URL: http://www.comsol.com.
[15] I.T. Jolliffe. *Principal Component Analysis*. Springer, 2nd edition, October 2002.
[16] The MathWorks. Matlab internet page. URL: http://www.mathworks.com.
[17] Maxime Barrault, Yvon Maday, Ngoc Cuong Nguyen, and Anthony T. Patera. An 'empirical interpolation' method: application to efficient reduced-basis discretization of partial differential equations. *Comptes Rendus Mathematique*, 339(9):667–672, November 2004.